A new experimental setup to measure hydraulic conductivity of plant segments

October 21, 2022

1 Abstract

Plant hydraulic conductivity and its decline under water stress is the focal point of current plant hydraulic research. Common methods of measuring hydraulic conductivity submit plant samples to conditions far away from those that are experienced in nature. In this paper, we present two methods for measuring hydraulic conductivity under closer to natural conditions, using suction to pull water through a plant sample while dynamically monitoring flow rate and pressure gradients. The novel setup presented here allows for controlling and rapidly changing flow and pressure conditions, enabling experimental assessment of rapid plant hydraulic responses to water stress. The setup also allows quantification of dynamic changes in water storage of plant samples. Our tests demonstrate that pulling water through a twig results in similar hydraulic conductivity values as the current standard method based on pushing water under high pressure. Surprisingly, further experiments revealed that hydraulic conductivity generally increases (slightly) with flow rate. Our experiments also revealed substantial contributions to flow by dynamic and largely reversible changes in the water storage of plant samples. At the same time, the setup allows easy detection and quantification of air intrusion due to leaks. Although the measurements can be performed under sub-atmospheric pressures, it is not possible to subject the samples to negative pressures due to cavitation inside the liquid phase. Regardless, this setup allows for unprecedented insights into the interplay between pressure, flow rate, hydraulic conductivity, and water storage in plant segments.

2 Background and Aims

Plant leaves absorb light and CO_2 for photosynthesis, but at the same time they lose water to the atmosphere through transpiration. To replenish water loss, plants entertain an elaborate network of xylem vessels that connect the water uptake tissues in the roots with the evaporating tissues in the leaves.

Similarly to porous media, water loss causes tension in the leaves, which drives root-leaf water transport along the pressure gradient between the leaves and the roots, supported by cohesion between water molecules. This is commonly described as the cohesion-tension theory (Dixon and Joly, 1895; Zimmermann et al., 1993; Tyree and Zimmermann, 2002; Shi et al., 2020).

Plant water transport through xylem can only be maintained if the pressure drop between roots and leaves is greater than the hydrostatic pressure drop due to the change in gravitational potential between roots and leaves. The drier the soil, the larger the tension in the soil itself, requiring even more tension (or lower water pressure) in the leaves to ensure water transport (Dixon and Joly, 1895). These pressures in the xylem are commonly so low that the system is believed to operate in a meta-stable state, where any disturbance or tiny air seeding in a vessel can cause cavitation, gas exsolution, or air seeding, resulting in embolisms, which would make a vessel dysfunctional for water transport (Sperry, 1986; Canny, 1998).

The presence of embolised vessels reduces the efficiency of water transport, expressed as a decrease in hydraulic conductivity. The reduced hydraulic conductivity due to embolism has to be compensated for by an increased pressure gradient, i.e. lower water pressures in the xylem, in order to maintain an adequate water transport role. The lower pressure leads to more cavitation and embolised vessels, resulting in the positive feedback loop of runaway cavitation (Tyree and Sperry, 1988; Hölttä et al., 2009).

Vulnerability of a plant to cavitation and cavitation's effect on hydraulic conductivity is the primary focus in current plant hydraulic research (McDowell et al., 2019). To quantify this vulnerability, hydraulic conductivity is determined experimentally by measuring the relationship between flow through a plant segment and the pressure drop along the flow path. After determining hydraulic conductivity under unstressed conditions (at 0 water potential, usually after flushing the plant segment with water under strongly positive pressure), the sample is subjected to increasing amounts of hydraulic stress, e.g. by bench dehydration or centrifugation of the sample (see below), and the reduction in

conductivity is measured repeatedly to produce a plot of percent loss of conductivity against the sample's water potential. Due to the focus on relative loss in conductivity, the absolute values of conductivity are commonly not reported. More in-depth information on the different methods for hydraulic conductivity and vulnerability measurements can be found in Cochard et al. (2013) and Venturas et al. (2017).

In the most common method for measuring plant hydraulic conductivity, one end of the plant sample is attached to a tube with above-atmospheric liquid pressure (e.g. a water reservoir that is elevated), while the other is exposed to atmospheric pressure, where water drips into a reservoir placed on a balance. The change in weight of the downstream reservoir over time is used to calculate the flow generated by the hydraulic head. In this paper we will refer to this method as the "Sperry method" (Sperry et al., 1988; Canny et al., 2007; Torres-Ruiz et al., 2012).

A similar technique to the Sperry method uses a high pressure flow meter (HPFM), where pressure is generated on one side using compressed air to push water through a plant sample connected by flexible tubing. The flow is calculated from the pressure drop across a capillary located between the plant sample and the pressure generator. In this paper we will refer to this method as the "HPFM setup" (Tyree et al., 1993). The HPFM setup is mainly used for measuring the hydraulic conductivity of roots (Tyree et al., 1995; Tsuda and Tyree, 2000).

In both Sperry and HPFM methods, the pressure difference along the sample is controlled (atmospheric at the outflow side of the twig and above-atmospheric at the inflow side), while the flow rate is a function of the hydraulic conductance of the twig. This is in contrast to natural conditions in a plant, where the system functions at negative liquid pressure and the pressure drop along the flow path is determined by the flow rate, i.e. the transpiration rate (Venturas et al., 2017).

A method that in theory enables conductivity measurements at negative liquid pressure is the Cavitron method (Alder et al., 1997; Cochard et al., 2013), where a plant sample with cuvettes on each end is placed in a centrifuge, and the pressure inside the twig is determined by the rotation rate of the centrifuge, whereas the pressure gradient depends on the position of water menisci in the cuvettes. The pressure along the twig is non-linear, with the lowest pressure in the middle (Cochard, 2002), rather than at the sink, as it would be in a real plant.

The water level of the downstream cuvette is fixed at the position of its

outflow hole, while the water level in the upstream cuvette is located further off-center, thus creating a pressure gradient between the two ends of the plant sample. During the experiment, the water level of the upstream cuvette slowly recedes as water is transported through the plant sample towards the downstream cuvette. The flow rate could be calculated by taking the change in water level in the upstream cuvette over time and multiplying it with the cross-sectional area of water in the cuvette. However, due to the unknown twig volume in the cuvette, an exact flow rate, and thus hydraulic conductivity, is not routinely determined, only the relative loss in conductivity is recorded as rotation speed is increased.

None of these methods can simulate vulnerability to runaway cavitation, as they all control the pressure gradient across plant samples such that in the event of cavitation, the flow rate decreases, not the pressure, as would be expected in an intact plant. In fact, except for the Cavitron method, all methods involve above-atmospheric pressures, so water stress cannot be induced while measuring hydraulic conductivity. Finally, none of the above methods quantifies changes in water storage of the plant sample, so it is not clear if the flow measured at one end of the sample constitutes through-flow or if part of the observed flow is due to emptying or re-filling water storage in the plant sample (Torres-Ruiz et al., 2012).

To fill these methodological gaps, in the present study, we aim to design an experimental setup for measuring hydraulic conductivity closer to natural conditions, with the following goals:

- Flow rate controlled, pressure drop as response;
- Suction-induced flow;
- Ability to simulate water stress in the plant segment;
- Ability to measure changes in storage.

3 Materials and Methods

Below, we present two different setups that were designed to achieve the above-mentioned goals. One is an intuitive, low-cost vertical setup resembling an artificial plant. The second is a more controlled horizontal setup, improving on certain shortcomings of the vertical setup.

3.1 Artificial Plant Setup

The initial setup was designed to mimic a plant in the simplest form, containing one evaporating "leaf", one "root" immersed in a water reservoir, and connecting tubes where a plant segment is inserted in a vertical setup (Fig. 1). The root and leaf each is replicated by a Rhizon sampler (Rhizosphere Research Products B.V., Wageningen, Netherlands), consisting of a membrane with pores of 5μm diameter. Pressure sensors (24PC; Honeywell, Morristown, NJ, USA) are connected through T-valves on either side of the plant segment. A liquid flow-meter (SLG-0150; Sensirion, Stäfa, Switzerland) is inserted in the flow path below the lower pressure sensor. The water reservoir consists of a beaker filled with de-ionized water.

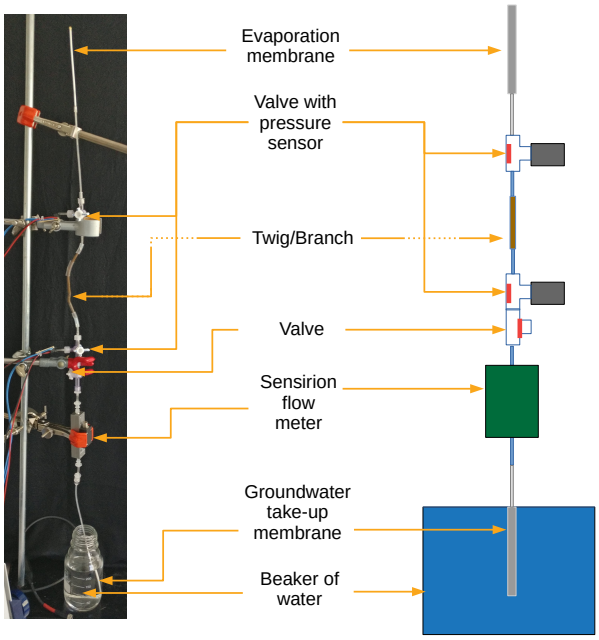

Figure 1: Setup for measuring hydraulic conductivity of twig samples using an evaporation membrane to drive flow.

Evaporation from the leaf replica generates the suction necessary to pull water up all the way from the beaker, following the cohesion-tension principle. Note that the membranes need to be covered by a continuous water film, otherwise air can enter through empty pores and water transpired at the surface is replaced by air, instead of water from below.

Initial filling of the system is performed without a twig in place, by placing both membranes in a beaker filled with DI water. A syringe is attached to one of the T-valves, at the position where the twig will be added. The syringe is pulled to fill the membrane and tubing with water. Turning the T-valve to only be open to the syringe and pressure sensor, the sensor is removed and water is pushed to fill that section and the sensor is re-attached. The process is repeated with the other side. Finally, the twig sample is attached and the setup is placed upright with one membrane in the beaker and the other held in the air using a stand where it begins to evaporate (Fig. 1).

3.2 Horizontal Syringe Setup

The horizontal syringe setup (Fig. 2) consists of a syringe pump (neMESYS; Cetoni, Wiesenring, Germany) to control the flow rate, a bypass around the twig connected with T-valves, pressure sensors on either side of the twig, and a flow meter (SLI-0430; Sensirion, Stäfa, Switzerland). Additionally, a capillary is connected between the water beaker and the flow meter to increase flow resistance on the upstream side and hence reduce overall pressure in the system if desired. A second bypass is present, such that flow can either go through or around the capillary.

The system is water filled by pulling water from the beaker to the syringe pump, then detaching the syringe to empty the air and re-attaching it.

This setup will be referred to as the "Syringe setup".

3.3 Calibration Procedure

In this section, we describe the calibration procedures for the pressure and flow sensors. The flow sensor is calibrated before each experiment as there can be instrument drift between experiments without cleaning. The drift is due to biological residue build-up within the sensor that requires flushing. Water flow is redirected through the bypass around the sample (Fig. 2f) with a direct path between the syringe and water reservoir. Known flow rates are generated using the syringe pump and correlated with measurements from the flow meter. The calibration is performed using a linear regression and applied to the data.

Pressure sensors are calibrated individually using the relation between pressure and volume using the ideal gas law. Initially we weigh an empty tube and t-valve to which the pressure sensor is attached, which we then fill with water and weigh again. By dividing the weight difference between them by the density

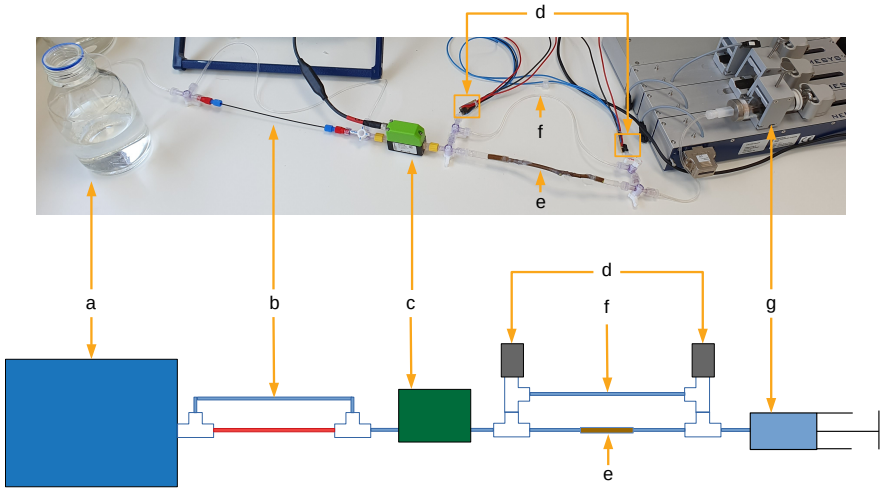

Figure 2: Horizontal syringe setup using syringe pump (g) to control water flow rate to and from the beaker (a). The twig (e) is inserted in the flow path to measure its hydraulic conductivity using flow (c) and pressure (d) meters. The bypass (f) is used to calibrate the sensors before an experiment. A capillary with bypass (b) is used as an example modification to lower the pressure.

of water, we obtain the internal volume, which is the initial gas volume. Then, a known change in volume is applied using the syringe and the corresponding pressure is calculated using the ideal gas law. The pressure is correlated to the measured voltage of the pressure sensor and its calibration function is determined using a linear regression. Before each experiment, the difference in pressure between the two sensors is measured at two points to remove any offsets. The first point is measured before an experiment when the sensors are at atmospheric pressure. The second point is the lowest attainable liquid pressure reachable with the setup, i.e. the water vapor pressure, which is measured once the experiment has concluded. The latter is measured by closing valves such that the syringe is only connected to both sensors via the bypass and flow cannot occur. The syringe is set to pull at 250 μL min^{-1}, and as in-flow is stopped, pressure lowers to the vapor pressure where gas bubbles form and the pressure no longer decreases. The flow is continued for 20 minutes. The wa-

ter vapor pressure measurement occurs after the experiment as the measuring process fills the setup with gas. From the two points, a linear regression of the difference between the pressure sensors is calculated and a correction is applied to remove their offset.

3.4 Sample Collection and Connection

All twig samples used in this paper are *Fagus sylvatica* collected in Belval, Luxembourg, following Wheeler et al. (2013) to avoid having any artificial cavitation in the sample. The branch is cut from the tree and left to sit in a bag for at least 30 minutes. The branch is then re-cut under water, cutting at least one vessel length from either side of the sample to make sure that any embolism due to the initial cut is removed. For samples in this paper, 10 cm are removed from each end, as Buchmüller (1986) found that 40% of the dry wood segments of Fagus sylvatica had a maximum vessel length of under 8 cm, with an additional 30% of samples having a maximal vessel length between 8 and 16 cm. Any branches along the cut segment are removed under water and sealed with parafilm and/or silicon gel as needed to seal for air seeding. Flexible tubing is attached to both ends of the submerged twig, then removed from the water and connected to either side of the setup. The diameter of the samples varied between 3.8 and 4.2 mm. We did not measure the diameter for all the samples, thus a value of 4.0 mm was used for the calculations (see below).

3.5 Conductivity Calculation

Flow through a porous medium such as the twig xylem can be described using Darcy's Law (Eq. 1):

$$Q_m = \frac{kA\rho}{\mu L}\Delta P \tag{1}$$

$$Q_V = \frac{Q_m}{\rho} \tag{2}$$

where Q_v is the volumetric flow rate ($m^3\ s^{-1}$), k is the intrinsic permeability (m^2), A is the cross sectional area of flow (m^2), ΔP is the pressure drop along the flow path (Pa), μ is the dynamic viscocity (Pa $\cdot$ s), and L is the length of the segment (m).

In literature, the efficiency of water transport through a twig sample is ex-

pressed in several different ways, as specific conductivity using $K_S = \frac{k}{\mu}$ (kg m^{-1} Pa^{-1} s^{-1}), as specific conductance which does not account for sample length, where $K_{AS} = \frac{k}{\mu L}$ (kg m^{-2} Pa^{-1} s^{-1}) (Caquet et al., 2009). In the case of Bär et al. (2018); Rosner et al. (2019), the units of the specific conductivity were reported as "m^2 Pa^{-1} s^{-1}", which are obtained when substituting the mass flow rate in Eq. 1 with the volumetric flow rate using Eq. 2.

In this chapter, we calculate the specific hydraulic conductivity of twig samples using the formulation from Sperry et al. (1988).

$$K = -\frac{Q_V \rho}{\Delta P} \frac{L}{A} \tag{3}$$

where K is the hydraulic conductivity (kg m^{-1} Pa^{-1} s^{-1}), ρ is the density of water (kg m^{-3}),

The pressure drop is measured by pressure sensors on both sides of the twig, as described above. The length of the twig is measured as the distance between the centers of the cuts on each side. The cross-sectional area (A) is calculated assuming a circular shape. The flow rate in the syringe setup is measured by both the syringe pump and the flow sensor. Unless otherwise noted, the flow meter measurements were used to calculate conductivity in this paper as these resulted in more stable values conductivity values (see also SI Fig. 2).

3.6 Experiments

Two experiments are presented for the artificial plant setup. In the first experiment, the setup was left to evaporate to test the measurement of flow, pressure difference, and conductivity change over time. Then, we attempted to produce runaway cavitation by adding a gas bubble to initiate embolism. The gas bubble was added through a valve below the lower pressure sensor and rose to the twig while flow, pressure, and hydraulic conductivity were being measured.

In the second experiment, the goal was to determine the lowest possible pressure that could be maintained by the artificial plant setup. To lower the pressure in the artificial plant setup as far as possible, the experiment was run without any sample and the valve connected to the lower pressure sensor was closed. As evaporation continued through the pores of the membrane, water menisci in the pores became progressively indented, creating suction and lowering the pressure until cavitation or air entry occurred. This procedure was repeated three times. The data of the upper pressure sensor was used for the experimental determination of the air entry value since it was closest to the

point of air entry.

The remaining experiments were conducted using the horizontal syringe pump setup. First, the setup was compared with the current standard, the Sperry method, to verify if similar values of hydraulic conductivity are obtained using either method. For direct comparison, both methods were applied consecutively using the same sample. The Sperry method was applied by disconnecting the syringe pump (g in Fig. 2), and letting the water drain freely while elevating the beaker at the other end of the setup (a in Fig. 2) to create the desired pressure difference. The chosen hydraulic head differences along the setup were 35.5, 73.5, and 104.9 cm. After this set of measurements, the beaker was placed back on the table, the syringe pump was re-attached, and water was pulled through the sample at flow rates of 10, 20, and 30 μL min^{-1}, to create similar pressure differences as in the previous Sperry method.

The next experiment was designed to simulate water stress in plants using the syringe setup. Two types of water stress were simulated, (a) reduced water supply (e.g. due to soil moisture drought), and (b) increased leaf water demand (e.g. in the mornings, or due to wind gusts or sunflecks). To simulate soil moisture drought, water flow between the beaker and the twig was deviated through a capillary by turning the valves in Part b of Fig. 2, resulting in increased flow resistance upstream of the twig and hence reduced pressure. Increased water demand was simulated by increasing the flow rate induced by the syringe pump, increasing the pressure gradient along the twig.

The final experiment was designed to quantify the change in twig water storage between a relaxed condition (zero flow, e.g. at night) and flow under tension (e.g. during the day). In this experiment, the syringe setup was started in the same way as in the soil moisture drought experiment, i.e. water was passed through a capillary before reaching the twig. When the measured flow rate into the twig became roughly steady, the syringe pump was stopped and the subsequent slow decay in flow rate was monitored until flow was no longer detected. Differences between syringe pump flow and the flow meter signal were interpreted as rate of change in twig storage.

Experiments were run in a ventilated lab around 21 °C and humidity between 25 and 40 %.

4 Results

4.1 Conductivity Measurement with Artificial Plant Setup

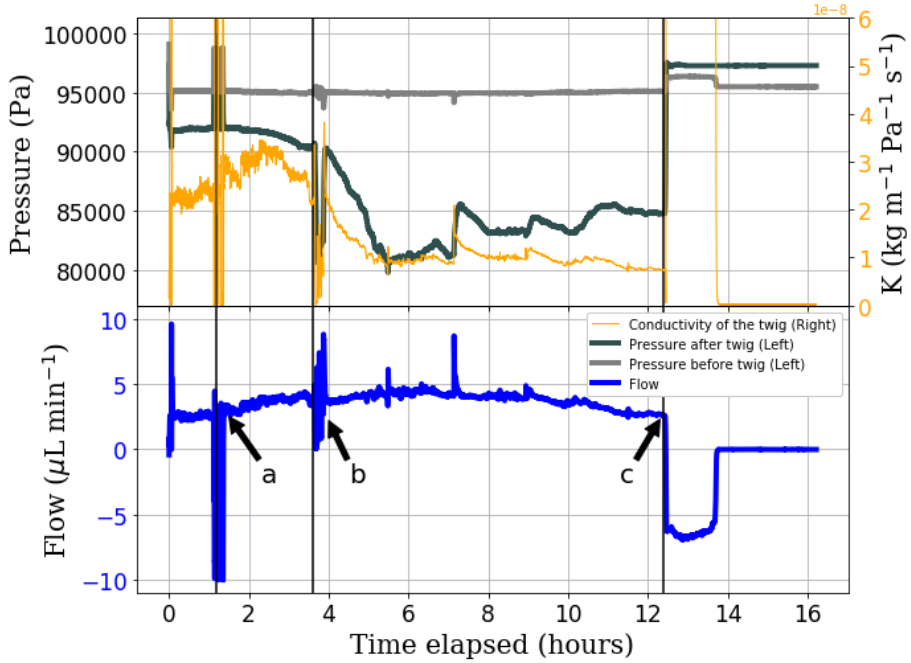

Figure 3: Flow, pressure, and conductivity measurements of a 2.2 cm Fagus sylvatica sample in the artificial plant setup. Air bubble was added below the lower pressure sensor 'a', and reached the sample at time 'b'. Air entered the membrane at the top and flow reversed at 'c'.

Time in the graphs begins at 0 with the start of the experiment, which represents the first time flow was induced. This was either when the membrane was removed from water, the beaker was moved to a higher elevation, or the flow was stared with the syringe pump.

A 2.2 cm long twig was attached to the artificial plant setup and left to evaporate. The flow rate started at 2.5 μL min^{-1} and increased steadily to 4.0 μL min^{-1} over the first 3.7 hours of the experiment. During this time, the pressure above the twig slowly decreased from 93 kPa to 91.5 kPa (Fig. 3). The conductivity of the sample increased from 2.3×10^{-8} to 2.5×10^{-8} kg m^{-1} Pa^{-1} s^{-1} over the first hour. The air bubble was added at 1.5 hours (Fig. 3a) while conductivity continued to increase to a peak of 3.3×10^{-8} kg m^{-1} Pa^{-1} s^{-1} at

the 2.3 hour point and then decreased again to 2.7×10^{-8} kg m^{-1} Pa^{-1} s^{-1} at 3.7 hours, when the bubble reached the sample. At this point, flow dropped to 0 and pressure decreased rapidly to 80.7 kPa (Fig. 3b), at which point the air bubble began passing through the twig. The pressure returned to the previous 91.5 kPa, and flow resumed at 4 μL min^{-1}. The flow remained relatively stable for the next 1.5 hours while both pressure and conductivity decreased markedly (from 91.5 kPa to 80.7 kPa and from 2.1×10^{-8} to 1.0×10^{-8} kg m^{-1} Pa^{-1} s^{-1}, respectively) during this time. Both pressure and conductivity stayed relatively steady for the next 6 hours until air entered the upper membrane from outside at 12.5 hours (Fig. 3c). The upper pressure increased and flow reversed, draining water from the setup above the twig, until the water meniscus stopped at the top of the twig.

The second experiment was conducted without a twig, just to determine the minimum sustainable liquid pressure in the system before air enters through the membrane. After the valve was closed, essentially blocking water supply while evaporation from the upper membrane was ongoing, the pressure kept decreasing until air entry occurred through the top membrane. Over three trials, air entered at pressures between 49.5 kPa and 56.9 kPa. When air entered through the top membrane, the flow direction reversed until all the water drained into the lower water reservoir.

4.2 Horizontal Syringe Setup vs. Sperry Method

In the first step, water was pushed through the twig sample using the Sperry method (Fig. 4a). Reservoir 'a' in Fig. 2 was elevated to 35.5 cm for 30 minutes, then to 73.5 cm for 30 minutes, then to 104.9 cm for 30 minutes, and then returned to 73.5 cm for another 30 minutes, before returning to 35.5 cm for 30 minutes.

In the second step, the syringe pump was re-attached and water was pulled through the sample at 10 μL min^{-1} for 30 minutes, then at 20 μL min^{-1} for 30 minutes, then at 30 μL min^{-1} for 30 minutes, then again at 20 μL min^{-1} for 30 minutes, before returning to 10 μL min^{-1} for another 30 minutes (Fig. 4b).

During the first 2.5 hours of the experiment, when the Sperry method was used (Fig. 4a), conductivity decreased steadily at constant head (from 6.0×10^{-7} to 2.0×10^{-7} kg m^{-1} Pa^{-1} s^{-1} overall). When the pressure gradient was increased at 0.5 hours, there was a step increase in conductivity from 3.6×10^{-7} to 4.1×10^{-7} kg m^{-1} Pa^{-1} s^{-1}. Similar increases in conductivity were observed

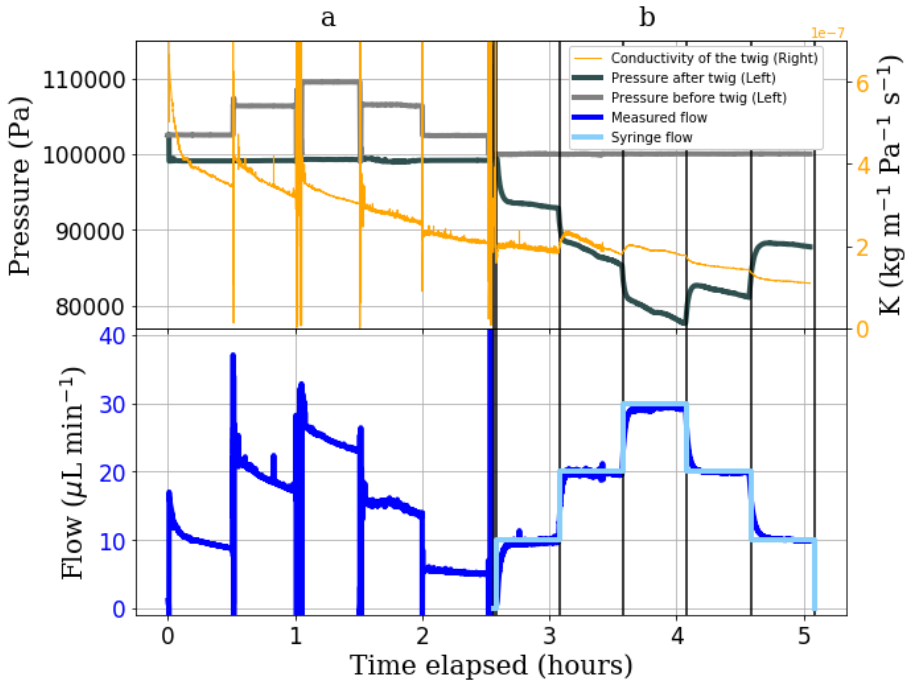

Figure 4: Pressure, flow, and conductivity measurements of a 10.2 cm twig sample over time. Section 'a' represents measurements when water is pushed through a twig sample using controlled pressure differences (Sperry method). Section 'b' represent measurements when water is pulled through the same sample in the same direction using a syringe pump (Syringe setup).

every time the pressure gradient was increased, but step decreases in pressure gradient did not have an evident effect on conductivity. Also when the method switched from Sperry method to Syringe at 2.5 hours, the hydraulic conductivity was not affected and remained at 2.1×10^{-7} kg m^{-1} Pa^{-1} s^{-1} during the transition. Over the 2.5 hours of the syringe pull (Fig. 4b), conductivity also decreased, but more slowly (from 2.1×10^{-7} to 1.1×10^{-7} kg m^{-1} Pa^{-1} s^{-1}). Whenever flow rate was increased, there was a step-wise increase in conductivity, and whenever flow rate was decreased, there was a slight step-wise decrease in conductivity.

When the different hydraulic heads where applied in the Sperry method (Fig. 4a), the pressure was constant and the flow rate decreased over time. However, when different flow rates were applied in the Syringe method (Fig. 4b), it was the pressure that decreased over time while flow was constant.

4.3 Simulating Water Stress

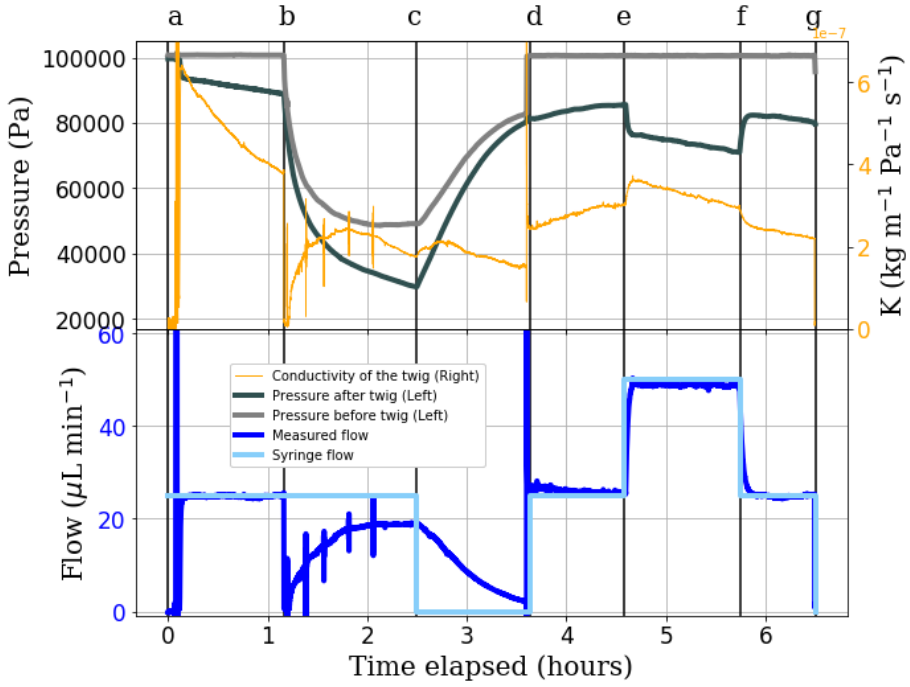

Figure 5: Time series of pressure, flow, and conductivity of a 13.5 cm twig when simulating different sorts of water stress. At 'a', a constant pull through the twig at 25 μL min^{-1} is applied and flow goes around the capillary. At 'b', flow is lead through a capillary upstream of the twig. At 'c', the syringe pump is stopped. At 'd', conditions are similar to 'a'. At 'e', flow is further increased to 50 μL min^{-1} and returned to 25 μL min^{-1} at 'f'. The experiment ends at 'g'.

In Fig. 5, the letters 'a' through 'g' indicate a change to the experimental setting. From 'a' to 'b', a constant pull was applied through the twig at 25 μL min^{-1} with no flow through the capillary, representing a steady evaporation of the leaf during the day at unrestricted water supply. This reference scenario was established in between the different stress scenarios for direct comparison to the reference state.

Drought stress is simulated at 'b', where flow was redirected through a capillary upstream of the twig. Flow initially stopped and pressure before the twig decreased sharply, followed by a decrease in pressure after the twig, and slow recovery of flow and conductivity, which reached 2.3×10^{-7} kg m^{-1} Pa^{-1} s^{-1} before declining again. When the syringe pump was stopped at 'c', flow decreased

from 19 to 3 μL min^{-1} over the course of an hour while pressures increased. Conductivity remained similar to that in Segment 'a-b', around 2.0×10^{-7} kg m^{-1} Pa^{-1} s^{-1}.

At 'd', the syringe pump was turned on again and the capillary bypassed, as in Segment 'a-b'. When the pump was turned on, flow rate increased instantly, accompanied by a step increase in conductivity from 1.5×10^{-7} to 2.6×10^{-7} kg m^{-1} Pa^{-1} s^{-1}. Note that the measured flow rate was initially even higher than the syringe pump flow rate in Segment 'd'.

Increase in water demand was simulated at 'e', where water flow through the twig was increased from 25 to 50 μL min^{-1}. The flow change was immediately reflected by the flow meter and pressure after the twig decreased suddenly from 85 kPa to 74 kPa, while the conductivity increased from 3.0×10^{-7} to 3.5×10^{-7} kg m^{-1} Pa^{-1} s^{-1}, followed by a steady decline back to 3.0×10^{-7} kg m^{-1} Pa^{-1} s^{-1}.

Once the original flow of 25 μL min^{-1} was re-established at 'f', pressure after the twig increased again to almost its original value at 'e', whereas conductivity showed another step decrease from 2.9×10^{-7} to 2.6×10^{-7} kg m^{-1} Pa^{-1} s^{-1}.

4.4 Twig water storage

To better understand if the deviations between syringe pump and flow meter flow rates observed in the previous experiment were related to changes in twig water storage, Segments 'a-d' were repeated with a new twig, but with a longer period without syringe pump flow at the end. Changes in storage were calculated as the cumulative difference between the flow rates at the syringe pump and the flow meter.

At the start of the storage experiment (Fig. 6 'a' to 'b'), the same pattern of declining conductivity as in the stress experiment was found. When the flow was passed through the capillary at 'b', the measured flow rate briefly declined to 0, followed by a steady recovery, reaching a steady rate of 21.7 μL min^{-1} at 'd', 3.3 μL min^{-1} lower than the syringe flow. Interpreting the difference in flow rates as a change in twig water storage, this would suggest that the amount of water in the twig decreased by 475 μL at 'd'. When the syringe pump was turned off ('d' to 'e') the flow meter kept recording flow into the twig, suggesting re-filling of the twig water storage until the flow ceased entirely after another 1.5 hours. At this point, our calculation would suggest a remaining twig water deficit of 175 μL (light blue line in bottom panel of Fig. 6).

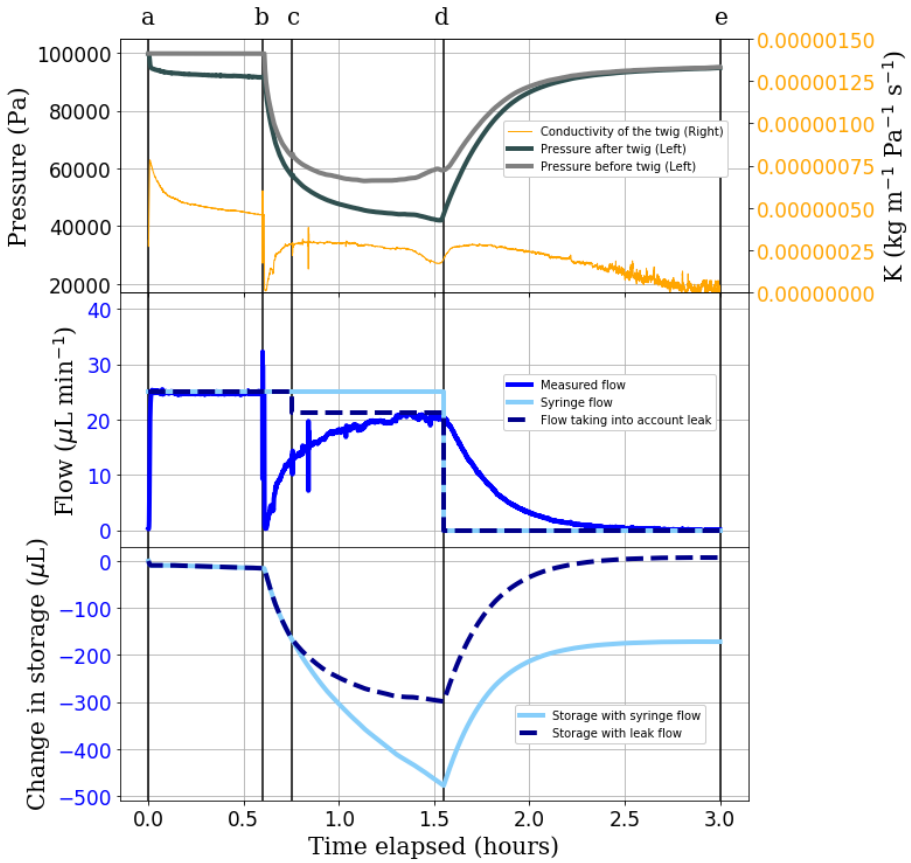

Figure 6: Graph of pressure, flow, conductivity, and storage changes when simulating water stress on a 11.4 cm twig. At 'a', a constant pull through the twig at 25 μL min^{-1} was applied and flow went around the capillary. At 'b', flow was lead through the capillary. At 'd', flow was stopped. The experiment ended at 'e'. Change in storage was calculated as the cumulative difference between measured flow and syringe flow. Air seeding was assumed to have formed at 'c', see main text.

The lower flow rate at 'd', along with a bubble seen in the syringe, indicated the presence of air seeding that was assumed to have formed at 'c' due to a kink in the pressure observed after re-analyzing the data. The air seeding is assumed constant from 'c' to 'd' and to be equal to the flow rate difference between the steady state flow at 'd' and the syringe flow. Using the flow rate based on the presence of the air seeding, storage would have decreased a maximum of 300 μL at 'd' and the end storage at 'e' would have been 7 μL larger than the initial

twig water storage at 'a'.

5 Discussion

In this paper we presented two different methods for measuring hydraulic conductivity under suction and flow-controlled conditions. Both methods are able to measure hydraulic conductivity during suction-induced flow. The first method, which we refer to as the artificial plant setup, consists of an artificial root (microporous membrane) dipped in a beaker of water or soil, and an artificial leaf (similar microporous membrane) exposed to the air and evaporating water. The twig sample is inserted in the vertical flow path between two pressure sensors that measure the pressure drop along the twig as flow is driven by suction exerted on the evaporating end. Simultaneously, a liquid flow meter records the flow, so that twig conductivity can be deduced from the pressure gradient and flow rate. In numerous experiments not shown here, we found that stable flow could be maintained for many hours in this setup, but invariably, sudden, catastrophic failure occurred by air entry through the evaporating microporous membrane after many hours. An interesting feature of this setup is its educational value, as its vertical orientation and components are intuitively associated with key macroscopic components of the plant hydraulic system. In our air seeding experiment, where we introduced an air bubble below the twig, we were able to see the sudden decline in liquid pressure on the leaf side as the bubble reached the twig, but then, surprisingly, as the pressure difference reached a threshold of 15,000 Pa (Fig. 3b), the bubble started entering the twig and pressure returned to its original value within tens of minutes. After 15 minutes we were able to observe air bubbles coming out of the twig on the upper side, indicating that at least part of the gas in the introduced bubble passed through the whole twig and left it again at the other end. Contrary to expectations that air seeding would lead to catastrophic failure of the hydraulic system, flow and evaporation continued at the original rate throughout this experiment, with only short-term perturbations when the bubble was introduced and when it passed through the twig. This was despite a marked decrease in hydraulic conductivity from 3.5×10^{-8} to 1.0×10^{-8} kg m^{-1} Pa^{-1} s^{-1} during the experiment. It is not clear if the decline in hydraulic conductivity was caused by the air seeding or independent of it, as the decreasing trend was observed before the bubble reached the twig, and the same trend continued after it had passed through the

twig. Note that the behaviour documented here was only observed with a twig that were shorter than its average xylem vessel length (here a twig of 2.2 cm was used, cf. an average xylem vessel length of under 8 cm for *Fagus sylvatica* (Buchmüller, 1986)). When a longer twig of 12.3 cm was used (data not shown), flow stopped as soon as the bubble reached the lower twig end after 4.2 hours and the bubble did not pass through the twig, leading to air entry through the evaporating membrane and failure after 5.9 hours (Found in SI Fig. 1). This also means that there was no vessel longer than 12.3 cm present in the sample.

This simple experiment taught us two important lessons, (a) evaporation and flow rate were not affected by changes in hydraulic conductivity, and (b) air seeding did not have a lasting effect on flow rate if continuous vessels were present in the twig (i.e. twig shorter than mean vessel length). The latter could suggest that the primary function of vessel ends and pit membranes is not to maintain flow, but actually to prevent gas from being transported upstream. In our setup, gas transported upstream accumulated at the top of the artificial leaf, creating to a pressure drop between the bulk water and the evaporating sites at the tip, eventually resulting in air entry at the top of the membrane.

The limit due to this air entry of the setup was tested in the second experiment. If the water pressure falls below a certain point, air enters through the membrane's pores and stop water from flowing to the top. The pressure difference required between the air and the liquid for air to enter is referred to here as the "air entry value". The expected air entry value for the membranes was calculated using a form of the Young-Laplace equation (Eq. 4) (Young, 1807).

$$P_{ae} = \frac{2\sigma_w}{r_p} \tag{4}$$

In Eq. 4, σ_w is the surface tension of water (N m^{-1}), r_p is the radius of the pores in the membrane (m), and P_{ae} is the air entry value (Pa). Taking a surface tension of water at 20^{o}C of 0.07286 N m^{-1} and a pore radius of 2.5×10^{-6} m, the expected air entry pressure would be 58288 Pa. The air entry pressure is the difference between the water and air interface in the pore of the membrane, meaning that the lowest pressure the water can attain before air entry is calculated from the difference between atmospheric air pressure and the air entry pressure. Thus, the theoretical lowest pressure the water in the membrane can reach is 43037 Pa.

In summary, the artificial plant setup had several drawbacks:

1. The distance between the pressure sensors changed with the length of each new twig. Due to the vertical orientation, the length changes the hydrostatic pressure difference between the sensors, which needs to be recorded and taken into account for conductivity calculations of every sample.

2. The lowest attainable liquid pressure before air entry was in theory 49.5 kPa, which is far from the vapor pressure of water at room temperature of 2.7 kPa, so the system cannot be run anywhere near critical cavitation conditions.

3. The flow rate cannot be controlled reliably and in a simple manner, as evaporation depends on radiative energy input, temperature, humidity and air movement around the evaporating membrane. The decrease in flow seen in Fig. 3 could be attributed to a decrease in temperature in the lab overnight, a change in the ventilation, or humidity.

These drawbacks led to the development of the horizontal syringe setup, which improves on the previous design by first placing the setup horizontally, and hence avoiding the offset between pressure sensors due to gravitational potential and ensuring that the pressure difference measured by the sensors does actually represent the pressure drop along the twig. Note that branches can grow horizontally, so a horizontal setup is not less "natural" than a vertical one. Secondly, replacement of the evaporation membrane by a syringe pump eliminates the pressure limitation due to the membrane's air entry pressure, and fluctuations in flow caused by fluctuations in evaporation from the membrane. For the same reason, the use of a rhizon on the water uptake side was also abandoned. The original idea was to place the rhizon in a porous material to simulate the reduced liquid pressure exerted by the soil, but with the rhizons used, the pressure could not be lowered below the air entry pressure of the membrane. Instead, a capillary was used to reduce pressure on receiving side of the twig. In addition, the syringe pump allows the flow rate to be precisely controlled through either suction or pushing, as opposed to the evaporation from the membrane. As mentioned above, our experience with the evaporation membrane taught us that the hydraulic conductivity of the system does not affect the evaporation rate, but the pressure gradient across the sample (Fig. 3). Therefore, an experimental setup with constant flow and adapting pressure gradient might represent natural conditions relatively well, where stomatal re-

sponse times easily exceed fluctuations in transpiration due to sunflecks or wind gusts (Schymanski et al., 2013).

The horizontal syringe setup and the Sperry method gave comparable values for hydraulic conductivity of the same sample (Fig. 4). Furthermore, the overall trend in the conductivity over time is maintained when swapping between the two methods. The step increase and decrease patterns, when changing pressure difference or flow rate, were seen in both methods, showing that the results are likely not of methodological nature, but biological. The specific hydraulic conductivity was measured between 6.0×10^{-7} and 2.0×10^{-7} kg m^{-1} Pa^{-1} s^{-1}, 3 to 4.5 times lower than literature values: 2.71×10^{-6} kg m^{-1} Pa^{-1} s^{-1} in (Bär et al., 2018) using the cavitron technique, 2.53×10^{-6} kg m^{-1} Pa^{-1} s^{-1} in Rosner et al. (2019) using the Sperry method, and 1.83×10^{-6} in the online database formed by Choat et al. (2012) (more xylem functional traits and measurements can be found at https://xylemfunctionaltraits.org/). The higher conductivity in the literature can be due to the filling of empty vessels when samples were flushed with water at high pressures leading to an increased conductive area.

The comparable hydraulic conductivity measurements between the Sperry method and the horizontal syringe setup, along with the similar results to literature confirm that the horizontal Syringe method is a valid alternative to the Sperry method for measuring hydraulic conductivity. In addition, the syringe setup was able to measure hydraulic conductivity while simulating water stress conditions. Simulated soil moisture stress caused a decrease in the pressure on both sides of the twig sample (Fig. 5), which is not possible using the Sperry or HPFM methods which rely on fixed pressure gradients and above-atmospheric pressure. Surprisingly, our experiment showed that an increase in flow rate increased the conductivity of the sample, both at constant pressure difference (Sperry method) and constant flow rate (Syringe method). The combination of both methods enables the conclusion that the sample's conductivity indeed depends on the flow rate, not just the pressure applied. This should be investigated on more species before speculating about a potential mechanistic explanation.

Another advantage of the syringe pump setup is that the flow rate is measured on both sides of the twig, giving additional information about the state of experiments. When pulling water through a sample, the water leaving the twig is determined by the syringe pump, while the flow entering the twig is measured by the liquid flow meter at the other end. In our experiments, it has enabled the detection of leaks or changes in the twig's storage (Fig. 6). The

following processes can cause a deviation between the measured flow (Q_m) and the syringe pump flow rate (Q_s):

1. Changes in water storage of the system between the flow meter and the syringe pump. This could result in $Q_m > Q_s$ or $Q_m < Q_s$.

2. Evaporation of water from the twig. This would result in $Q_m > Q_s$.

3. Air seeding or exsolution of gas between the flow meter and the syringe pump. This would result in $Q_m < Q_s$. Air bubbles should become visible in the tubes or the syringe pump in this case

Since we never observed persistently greater flow meter values compared to the syringe pump, we can exclude a significant contribution of 2. The only occurrences of $Q_m > Q_s$ were found for a limited time after reductions in flow rate, implicating changes in storage as the reason. In two cases, we documented persistently $Q_m < Q_s$, both under conditions of low pressure, and associated with the accumulation of gas in the syringe, indicating that air might have been present, or exsolution of gas due to low pressure. In general, if Q_m deviates from Q_s but then converges, this indicates that the system storage is adjusting to a new steady state. In Figs. 5 and 6, we found clear indications of changes in storage, some of which were followed by indications of temporary leaks or gas exsolution periods (persistently $Q_m < Q_s$ in Fig. 5b-c, and Fig. 6c-d). In Fig. 6, we calculated the change in storage from the cumulative sum of $Q_s - Q_m$ and used the steady value of $Q_s - Q_m$ in Fig. 6c to quantify the air seeding rate. Remarkably, when accounting for the temporary air seeding rate, assumed to occur only at a liquid pressure below 55 kPa (based on a slight bump in the pressure and flow data at this threshold), the storage deficit gradually returned to zero 1.5 hours after switching the syringe pump off, indicating the capacity of the twig to reversibly reduce and replenish its storage depending on the flow rate and pressure applied. Additional factors can be taken into account when calculating the twig storage, such as the effect of the flexible tubing not fully returning to original size, and the actual volume of air entering the system which changed due to changing pressure. These calculations can partially be found in the SI (Found in SI Fig. 3), as they go beyond the scope of this paper. This elastic storage component may also be the reason for the so-called 'passive water uptake' commonly found when using the Sperry method, which is then subtracted from the measured flow rates to achieve more consistent results (Torres-Ruiz et al., 2012). Since the magnitude of the 'passive water uptake'

increases with the xylem tension prior to the experiment (Table 1 in Torres-Ruiz et al., 2012), it is likely that the underlying mechanism is the same as that causing water flow into the twig at zero syringe pump flow rate after the water stress treatments (Figs. 5 and 6). The dynamic decay of this spontaneous water uptake observed in our experiments is consistent with the interpretation that it is likely related to a relaxation of elastic tissues (Zweifel et al., 2001). However, since the dynamics of flow during a conductivity measurement is usually not reported, we cannot tell in how far the 'passive water uptake' analysed by Torres-Ruiz et al. (2012) is indeed related to the elastic relaxation seen in our experiments, and if it was, how a constant rate of 'passive water uptake' could be deduced from such a dynamically decaying curve. Fortunately, the ability to measure flow rate on both sides of the twig in our setup gives us a clear indication of any artifacts in the flow measurements, and to our surprise, conductivity calculations based on the measured flow rate of water into the twig and the pressure gradient along the twig produced consistent conductivity values even during moderate emptying or re-filling of the twig water reservoir (see e.g. conductivity values before and after Point d in Fig. 6). The elastic relation of the setup without the twig was also tested to rule out setup artifacts and shows that the change in storage is an order of magnitude smaller without a twig, whereas even there, contraction is not fully reversible (SI Fig. 3 and 4).

The experiments presented here were not designed to gain any particular scientific insights, but to illustrate the capabilities and potential limitations of the newly presented methods. The main limitation of both methods is that the liquid pressure cannot be lowered sufficiently to induce significant loss of conductivity during a flow measurement. Even if the valve upstream of the twig is closed while the syringe pump is sucking, liquid pressure only decreases down to the saturation vapour pressure of the water in the tubes, i.e. around 3000 Pa at 25 °C, at which point cavitation occurs, triggered by any gas bubble in the system, including those inside the pressure sensors. Conducting flow and pressure measurements below this pressure, or even at negative pressures in the MPa range, as expected in plants, would require removal of all gas bubbles and any cavitation nuclei in the system, which has so far only been achieved in microscopic systems (Wheeler and Stroock, 2008; Pagay et al., 2014). Nevertheless, even at the modest range of sub-atmospheric pressures attainable in the current setup, we have been able to observe transient changes in twig water storage lasting for up to an hour, suggesting that this setup could be used to not only measure the hydraulic conductivity of plant segments very accurately,

but also gain a better understanding of the role of water storage in the plant hydraulic system.

6 Conclusion

Current methods of measuring hydraulic conductivity of plant segments are based on controlling a pressure gradient and pushing water through samples, which does not reflect natural water transport processes in plants, i.e. suction-driven flow with a pressure gradient determined by the flow rate imposed by leaf water demand. Here we describe two new experimental approaches to measure hydraulic conductivity using suction and a controlled flow rate. The artifical plant setup, consisting of an artificial root, an artificial leaf and a plant segment in the flow path between the two, is well suited for educational purposes, as its components are intuitively comparable to real plant components, whereas the syringe pump setup, oriented horizontally, where the evaporating artificial leaf is replaced by a syringe pump, is more versatile for conducting scientific experiments. Due to the use of a flow meter before the twig and syringe pump controlled suction at the other end, the setup enables detecting leaks in the system and also changes in twig water storage.

Our detailed tests of the setup confirmed that the conductivity values obtained are similar to those measured with the traditional Sperry method when similar flow rates are used. However, due to the ability to control flow in our setup, we found a positive correlation between flow rate and conductivity, which seems counter-intuitive, as we expected higher flow rates and the associated reduction in pressure to result in reduced hydraulic conductivity. Furthermore, our tests revealed that increases in flow resistance at the source or flow rate at the sink both result in transient withdrawal of water from the twig, which is largely reversible, i.e. the twig replenishes its storage to the original value when original flow conditions are restored. This enables unique insights into the interplay between pressure, flow rate, hydraulic conductivity and water storage in plant segments.

7 Data availability

All data and analysis code will be published on zenodo.org and at https://renkulab.io upon publication.

References

Alder, N. N., Pockman, W. T., Sperry, J. S., and Nuismer, S. (1997). Use of centrifugal force in the study of xylem cavitation. *Journal of Experimental Botany*, 48(3):665–674.

Bär, A., Nardini, A., and Mayr, S. (2018). Post-fire effects in xylem hydraulics of Picea abies, Pinus sylvestris and Fagus sylvatica. *New Phytologist*, 217(4):1484–1493. Publisher: John Wiley & Sons, Ltd.

Buchmüller, K. S. (1986). Jahrringcharakteristik und Gefässlängen in Fagus sylvatica L.I. *Vierteljahrsschrift der Naturforschenden Gesellschaft in Zürich*, 131(3):161–182.

Canny, M. J. (1998). Transporting water in plants. *American Scientist*, 86:152–159.

Canny, M. J., Sparks, J. P., Huang, C. X., and Roderick, M. L. (2007). Hypothesis: Air embolisms exsolving in the transpiration water–the effect of constrictions in the xylem pipes. *Functional plant biology*, 34(2):95–111.

Caquet, B., Barigah, T. S., Cochard, H., Montpied, P., Collet, C., Dreyer, E., and Epron, D. (2009). Hydraulic properties of naturally regenerated beech saplings respond to canopy opening. *Tree Physiology*, 29(11):1395–1405. Publisher: Oxford Academic.

Choat, B., Jansen, S., Brodribb, T. J., Cochard, H., Delzon, S., Bhaskar, R., Bucci, S. J., Feild, T. S., Gleason, S. M., Hacke, U. G., Jacobsen, A. L., Lens, F., Maherali, H., Martínez-Vilalta, J., Mayr, S., Mencuccini, M., Mitchell, P. J., Nardini, A., Pittermann, J., Pratt, R. B., Sperry, J. S., Westoby, M., Wright, I. J., and Zanne, A. E. (2012). Global convergence in the vulnerability of forests to drought. *Nature*, 491(7426):752–755. Number: 7426 Publisher: Nature Publishing Group.

Cochard, H. (2002). A technique for measuring xylem hydraulic conductance under high negative pressures. *Plant, Cell & Environment*, 25(6):815–819. _eprint: https://onlinelibrary.wiley.com/doi/pdf/10.1046/j.1365-3040.2002.00863.x.

Cochard, H., Badel, E., Herbette, S., Delzon, S., Choat, B., and Jansen, S. (2013). Methods for measuring plant vulnerability to cavitation: a critical review. *Journal of Experimental Botany*, 64(15):4779–4791.

Dixon, H. H. and Joly, J. (1895). On the ascent of sap.

Hölttä, T., Cochard, H., Nikinmaa, E., and Mencuccini, M. (2009). Capacitive effect of cavitation in xylem conduits: results from a dynamic model. *Plant, Cell & Environment*, 32(1):10–21.

McDowell, N. G., Brodribb, T. J., and Nardini, A. (2019). Hydraulics in the 21 st century. *New Phytologist*, 224(2):537–542.

Pagay, V., Santiago, M., Sessoms, D. A., Huber, E. J., Vincent, O., Pharkya, A., Corso, T. N., Lakso, A. N., and Stroock, A. D. (2014). A microtensiometer capable of measuring water potentials below -10 MPa. *Lab on a Chip*, 14(15):2806–2817. Publisher: The Royal Society of Chemistry.

Rosner, S., Heinze, B., Savi, T., and Dalla-Salda, G. (2019). Prediction of hydraulic conductivity loss from relative water loss: new insights into water storage of tree stems and branches. *Physiologia Plantarum*, 165(4):843–854. Publisher: John Wiley & Sons, Ltd.

Schymanski, S. J., Or, D., and Zwieniecki, M. (2013). Stomatal Control and Leaf Thermal and Hydraulic Capacitances under Rapid Environmental Fluctuations. *PLoS ONE*, 8(1):e54231.

Shi, W., Dalrymple, R. M., McKenny, C. J., Morrow, D. S., Rashed, Z. T., Surinach, D. A., and Boreyko, J. B. (2020). Passive water ascent in a tall, scalable synthetic tree. *Scientific Reports*, 10(1).

Sperry, J. S. (1986). Relationship of Xylem Embolism to Xylem Pressure Potential, Stomatal Closure, and Shoot Morphology in the Palm Rhapis excelsa 1. *Plant Physiology*, 80(1):110–116.

Sperry, J. S., Donnelly, J. R., and Tyree, M. T. (1988). A method for measuring hydraulic conductivity and embolism in xylem. *Plant, Cell & Environment*, 11(1):35–40.

Torres-Ruiz, J. M., Sperry, J. S., and Fernández, J. E. (2012). Improving xylem hydraulic conductivity measurements by correcting the error caused by passive water uptake. *Physiologia Plantarum*, 146(2):129–135. _eprint: https://onlinelibrary.wiley.com/doi/pdf/10.1111/j.1399-3054.2012.01619.x.

712 Tsuda, M. and Tyree, M. T. (2000). Plant hydraulic conductance measured by
713 the high pressure flow meter in crop plants. *Journal of Experimental Botany*,
714 51(345):823–828.

715 Tyree, M. T., Patiño, S., Bennink, J., and Alexander, J. (1995). Dynamic
716 measurements of roots hydraulic conductance using a high-pressure flowmeter
717 in the laboratory and field. *Journal of Experimental Botany*, 46(1):83–94.

718 Tyree, M. T., Sinclair, B., Lu, P., and Granier, A. (1993). Whole shoot hydraulic
719 resistance in Quercus species measured with a new high-pressure flowmeter.
720 *Annales des Sciences Forestières*, 50(5):417–423. Publisher: EDP Sciences.

721 Tyree, M. T. and Sperry, J. S. (1988). Do Woody Plants Operate Near the
722 Point of Catastrophic Xylem Dysfunction Caused by Dynamic Water Stress?:
723 Answers from a Model. *Plant Physiology*, 88(3):574–580.

724 Tyree, M. T. and Zimmermann, M. H. (2002). The Cohesion-Tension Theory
725 of Sap Ascent. In Tyree, M. T. and Zimmermann, M. H., editors, *Xylem*
726 *Structure and the Ascent of Sap*, Springer Series in Wood Science, pages 49–
727 88. Springer, Berlin, Heidelberg.

728 Venturas, M. D., Sperry, J. S., and Hacke, U. G. (2017). Plant xylem
729 hydraulics: What we understand, current research, and future chal-
730 lenges. *Journal of Integrative Plant Biology*, 59(6):356–389. _eprint:
731 https://onlinelibrary.wiley.com/doi/pdf/10.1111/jipb.12534.

732 Wheeler, J. K., Huggett, B. A., Tofte, A. N., Rockwell, F. E., and
733 Holbrook, N. M. (2013). Cutting xylem under tension or supersatu-
734 rated with gas can generate PLC and the appearance of rapid recovery
735 from embolism. *Plant, Cell & Environment*, 36(11):1938–1949. _eprint:
736 https://www.onlinelibrary.wiley.com/doi/pdf/10.1111/pce.12139.

737 Wheeler, T. D. and Stroock, A. D. (2008). The transpiration of water at negative
738 pressures in a synthetic tree. *Nature*, 455(7210):208–212.

739 Young, T. (1807). *A Course of Lectures on Natural Philosophy and the Mechan-*
740 *ical Arts: In Two Volumes*. Johnson. Google-Books-ID: lmM_AAAAcAAJ.

741 Zimmermann, U., Haase, A., Langbein, D., and Meinzer, F. (1993). Mecha-
742 nisms of Long-Distance Water Transport in Plants: A Re-Examination of
743 Some Paradigms in the Light of New Evidence. *Philosophical Transactions:*
744 *Biological Sciences*, 341(1295):19–31.

745 Zweifel, R., Item, H., and Häsler, R. (2001). Link between diurnal stem radius
746 changes and tree water relations. *Tree Physiology*, 21(12-13):869–877.